

Simultaneous detection of CH_4 and CO_2 through dual modulation off-axis integrated cavity output spectroscopy

Yi-Xuan Liu(刘艺璇), Zhou-Bing Wang(王周兵), Xin-Xin Wei(韦欣欣), Jing-Jing Wang(王静静), Xin Meng(孟鑫), and Gui-Lin Mao(毛桂林)

Citation: Chin. Phys. B, 2023, 32 (**10**): 104209. DOI: 10.1088/1674-1056/acdac1
Journal homepage: http://cpb.iphy.ac.cn; http://iopscience.iop.org/cpb

What follows is a list of articles you may be interested in

Anti-symmetric sampled grating quantum cascade laser for mode selection

Qiangqiang Guo(郭强强), Jinchuan Zhang(张锦川), Fengmin Cheng(程凤敏), Ning Zhuo(卓宁), Shenqiang Zhai(翟慎强), Junqi Liu(刘俊岐), Lijun Wang(王利军),Shuman Liu(刘舒曼), and Fengqi Liu(刘峰奇)
Chin. Phys. B, 2023, 32 (**3**): 034209. DOI: 10.1088/1674-1056/ac7291

A pressure-calibration method of wavelength modulation spectroscopy in sealed microbial growth environment

Kun-Yang Wang(王坤阳), Jie Shao(邵杰), Li-Gang Shao(邵李刚), Jia-Jin Chen(陈家金), Gui-Shi Wang(王贵师), Kun Liu(刘琨), and Xiao-Ming Gao(高晓明)
Chin. Phys. B, 2021, 30 (**5**): 054203. DOI: 10.1088/1674-1056/abda32

Absorption linewidth inversion with wavelength modulation spectroscopy

Yue Yan(颜悦), Zhenhui Du(杜振辉), Jinyi Li(李金义), Ruixue Wang(王瑞雪)
Chin. Phys. B, 2018, 27 (**2**): 024205. DOI: 10.1088/1674-1056/27/2/024205

Wavelength modulation spectroscopy for measurements of gas parameters in combustion field

Dong-Sheng Qu(屈东胜), Yan-Ji Hong(洪延姬), Guang-Yu Wang(王广宇), Hu Pan(潘虎)
Chin. Phys. B, 2017, 26 (**6**): 064207. DOI: 10.1088/1674-1056/26/6/064207

Wavelength modulation spectroscopy at 1530.32 nm for measurements of acetylene based on Fabry-Perot tunable filter

Yun-Long Li(李运龙), Bing-Chu Yang(杨兵初), Xue-Mei Xu(许雪梅)
Chin. Phys. B, 2016, 25 (**2**): 024208. DOI: 10.1088/1674-1056/25/2/024208

Simultaneous detection of CH_4 and CO_2 through dual modulation off-axis integrated cavity output spectroscopy

Yi-Xuan Liu(刘艺璇), Zhou-Bing Wang(王周兵), Xin-Xin Wei(韦欣欣), Jing-Jing Wang(王静静)[†], Xin Meng(孟鑫), and Gui-Lin Mao(毛桂林)[‡]

School of Physics and Electronic Engineering, Jiangsu Normal University, Xuzhou 221116, *China*

(Received 30 March 2023; revised manuscript received 16 May 2023; accepted manuscript online 2 June 2023)

This study established a novel method for the simultaneous detection of two-component gases. Radio frequency (RF) white noise disturbance laser current and wavelength modulation were simultaneously used to improve the off-axis integrated cavity output spectroscopy technique, and a high-precision dual modulation OA-ICOS (RF-WM-OA-ICOS) system was established. The two laser beams were coupled into one laser beam that was applied incident to the cavity of RF-WM-OA-ICOS system. The second harmonic signals of CH_4 and CO_2 gas simultaneously appeared in the rising or falling edge of a triangular wave. This method was used to measure CH_4 and CO_2 with different concentrations. The results indicated that the proposed system has high stability and can accurately and simultaneously measure the concentrations of CH_4 and CO_2, with an optimal integration time of 220 s. The minimum detection limit was 10 ppb for CH_4 and 1.5 ppm for CO_2. The corresponding noise equivalent absorption sensitivity values were calculated as 2.67×10^{-13} cm^{-1}·Hz$^{-1/2}$ and 5.18×10^{-11} cm^{-1}·Hz$^{-1/2}$, respectively. The proposed dual-component gas simultaneous detection method can also be used for high-precision simultaneous detection of other gases. Therefore, this study may serve as a reference for developing portable multicomponent gas analyzers.

Keywords: off-axis integrated cavity output spectroscopy, wavelength modulation, radio frequency (RF) white noise, simultaneous detection

PACS: 42.68.Ca, 07.88.+y, 42.62.Fi, 95.85.Jq **DOI:** 10.1088/1674-1056/acdac1

1. Introduction

Climate change is a major global issue and can be attributed to global warming, primarily caused by greenhouse gas emissions from human activities. According to the "State of the Global Climate 2021" report released by the World Meteorological Organization (WMO), the atmospheric concentrations of CO_2, N_2O, and especially CH_4 reached record highs in 2021 and continued to rise in 2022.[1] CH_4 and CO_2 are the critical greenhouse gases. The WMO has continuously measured their atmospheric concentrations at more than 100 monitoring sites worldwide over many years. The findings indicated that CO_2 concentration has increased since 1750, with an increase of 2.5 ppm to 415.5 ppm only in 2021. Furthermore, CH_4 increased by 18 ppb to 1908 ppb in 2021, more than 2.5 times the pre-industrial level.[2] Accurately detecting atmospheric greenhouse gases is crucial to environmental monitoring and sustainable human development. In particular, highly sensitive, multi-component, real-time *in-situ* detection technologies will contribute to the research and management of environmental problems in local areas.

Off-axis integrated cavity output spectroscopy (OA-ICOS)[3,4] is a notable method used for the detection of trace gases. It has attracted considerable research attention recently because of its simple structure, high system stability, and ability to be easily integrated. In OA-ICOS, light is reflected multiple times between mirrors by injecting an off-axis beam into a high-precision optical resonance cavity with an effective optical absorption path of 1 km–30 km. This method can effectively enhance absorption signals but introduces cavity mode noise, which is the primary noise in an OA-ICOS system. In theory, cavity mode noise decreases with the distance of the incident beam from the cavity axis. Therefore, cavity mode noise can be eliminated by using a sufficiently large high-reflection lens to build an optical cavity; however, this solution is not feasible in practical applications. In recent years, some studies have injected radio frequency (RF) white noise into laser beams to achieve current disturbance, effectively suppressing cavity mode noise; this method has increasingly attracted research attention. Ciaffoni *et al.*[5] injected filtered 30-MHz RF noise into a 764-nm vertical-cavity surface-emitting laser, resulting in a fourfold increase in the sensitivity of the oxygen sensor and an average minimum detectable absorption of 4.3×10^{-5} within a sampling time of 1 s. Manfred *et al.*[6] increased the laser linewidth effectively by applying a broadband RF noise into a mid-infrared quantum cascade laser to observe CO_2 absorption near 1890 cm^{-1} with an average minimum detectable absorption of 5.5×10^{-3} Hz$^{-1/2}$ within a sampling time of 100 ms. Shao *et al.*[7] used −25-dBm RF white noise to achieve laser current disturbance for the simultaneous detection of N_2O and CO with 350-ppb concentra-

[†]Corresponding author. E-mail: jin16217@mail.ustc.edu.cn
[‡]Corresponding author. E-mail: maoguilin@jsnu.edu.cn

© 2023 Chinese Physical Society and IOP Publishing Ltd

tions. The standard deviation (SD) of the direct absorption spectra after noise addition was improved by approximately 1.6 times compared with that without RF noise.

To improve detection sensitivity, OA-ICOS is often combined with wavelength modulation spectroscopy (WMS) as WM-OA-ICOS to further reduce the noise related to low-frequency fluctuation ($1/f$ noise) in the laser intensity and in the detection chain. Kasyutich *et al.*[8] reported the detection of the second harmonic ($2f$) signal of O_2 near 687.1 nm using the WM-OA-ICOS technique. The detection sensitivity of this method was seven times higher than that achieved by directly detecting the intensity of the integrated cavity output signal. Zhao *et al.*[9] reported that the signal-to-noise ratio (SNR) of WM-OA-ICOS (with a detection sensitivity of 3.6 ppmv·Hz$^{-1/2}$) was higher than that of OA-ICOS by 14 times. Wang *et al.*[10] simultaneously applied wavelength modulation and RF white noise in OA-ICOS and improved the system detection limit by more than six times. In addition, this method eliminated cavity mode noise while suppressing background noise in the system, further improving the detection limit for trace gases.

With the exacerbation of existing atmospheric problems, detecting single gas components cannot satisfy research requirements. To this end, the simultaneous detection of two-component or multicomponent gases is crucial to advancing existing environmental monitoring techniques. Dong *et al.*[11] used optical switching with membrane separation technology to construct a set of test prototypes for the simultaneous measurement of CH_4 and CO_2 dissolved in seawater, with detection limits of 0.56 ppb and 0.62 ppm, respectively. Wang *et al.*[12] realized the simultaneous measurement of atmospheric CO_2 and CH_4 by using a "dual-channel laser" mechanical structure combined with an off-axis integrated cavity. In addition, time-division multiplexing was used to separate the signals emitted by the dual-channel laser light source. The method required additional supporting hardware and software design, and the SDs of the original concentrations of CO_2 and CH_4 were 0.278 ppm and 1.794 ppb, respectively.

In the present study, high-precision simultaneous detection of two-component gases was realized by using OA-ICOS combined with RF white noise modulation and wavelength modulation (RF-WM-OA-ICOS) and a dual-channel beam combiner. Accordingly, an RF-WM-OA-ICOS system was constructed to detect CH_4 and CO_2 simultaneously, and the performance of the system was evaluated.

2. Basic principle of RF-WM-OA-ICOS

Cavity mode noise in OA-ICOS is attributable to the coherence of laser light.[13–15] The narrower the laser bandwidth, the better the coherence of the laser. When a laser beam is incident on a resonant cavity, it reflects multiple times between two highly reflective lenses, resulting in many concurrent beams in the cavity and an increase in effective optical paths. If a laser beam is incident along the cavity axis, all reflected beams are aligned with the cavity axis. Thus, all the reflected beams coincide with each other, resulting in coherent superposition. Meanwhile, only a few cavity mode outputs, with each cavity mode having high light intensity.[13] These cavity modes cause severe noise in the absorption spectrum. If the laser is incident off-axis, the coincidence rate between the reflected beams decreases, and the probability of correlated superposition also decreases.[14] More cavity mode outputs are produced, decreasing the average energy of the cavity modes. When the output cavity mode density is sufficiently high, the energy of each cavity mode decreases to a considerably small value, suppressing the cavity mode noise. The coherent superposition effect and cavity mode noise also increase with the coherence of the laser.[15] When the coherence of the laser is low, the coherent superposition effect is not prominent, meaning that the cavity mode noise is suppressed. When the control current of the laser is interfered by RF white noise, the output laser linewidth increases; simultaneously, the coherence of the laser decreases.[16,17] The mutual interference between the laser beams decreases, and the cavity mode noise is suppressed because of the reduced coherence of the laser beams. In particular, when the laser linewidth is larger than the free spectral range, the cavity mode tends to disappear, and the output signal appears continuous, making the optical cavity equivalent to the traditional optical multi-pass cell.[18,19]

When a laser beam with an intensity of I_0 and a frequency of ν passes through an absorbing medium with a thickness of L, the intensity of the transmitted beam is low because of the partial absorption of light energy by the medium. The intensity of light decreases with the concentration of the absorbing medium. The intensity of the transmitted light can be expressed as follows:[13]

$$I(\nu) = I_0 \, \mathrm{e}^{-\sigma(\nu)NL}, \tag{1}$$

where $\sigma(\nu)$ and N denote the absorption cross-section of the absorbing molecules (cm^2·molecule^{-1}) and molecular number density (molecule·cm^{-3}), respectively. When a laser beam is incident off-axis on the cavity and the one-way absorption loss is considerably smaller than the cavity lens loss ($\sigma(\nu)NL_\mathrm{c} \ll 1-R$), the effective absorption optical path (L_eff) obtained can be expressed as

$$L_\mathrm{eff} = \frac{L_\mathrm{c}}{1-R}, \tag{2}$$

where L_c denotes the distance between the lenses that constitute the cavity. A modulating current $i(t)$ with a cosine signal of frequency f on it can be expressed as follows:[20]

$$i(t) = i_0 + a_\mathrm{m}\cos(2\pi f t), \tag{3}$$

where i_0 and $a_{\rm m}$ denote the center current and amplitude of the modulating laser signal, respectively. The modulation of the current results in a corresponding frequency modulation. The instantaneous frequency of the output signal can be expressed as

$$\nu = \nu_0 + a_\nu \cos(\omega t), \tag{4}$$

where ν_0 and a_ν denote the center frequency and amplitude of the modulated signal, respectively. Because both the modulating current and the detection signal are periodic functions, equation (4) can be expressed as a Fourier series,[21] and its harmonic components ν_n can be expressed as

$$\begin{aligned}\nu_n(\omega_{\rm L}) &= \frac{2I_0}{\pi}\int_0^{\pi}(\omega_{\rm L}+a_\omega\cos\theta)\\ &\quad\times {\rm e}^{-\sigma NL(\omega_{\rm L}+a_\omega\cos\theta)}\cos n\theta\,{\rm d}\theta\\ &= \frac{2I_0}{\pi}\int_0^{\pi}{\rm e}^{-\sigma NL(\omega_{\rm L}+a_\omega\cos\theta)}\cos n\theta\,{\rm d}\theta. \end{aligned}\tag{5}$$

When the gas is weakly absorbed to the ppm scale and $\sigma NL \ll 1$, equation (5) can be simplified as

$$\begin{aligned}\nu_n(\omega_{\rm L}) &= \frac{2I_0NL}{\pi}\int_0^{\pi}-\sigma(\omega_{\rm L}+a_\omega\cos\theta)\cos n\theta\,{\rm d}\theta\\ &= \frac{2^{1-n}I_0NL}{n!}a_\omega^n\frac{{\rm d}^n\sigma}{{\rm d}\omega^n}\,|\,\omega=\omega_{\rm L}. \end{aligned}\tag{6}$$

According to Eq. (6), the amplitude of the harmonic component $2I_0NL/\pi$ is proportional to the absorption molecule concentration when the effective absorption optical range L is held constant. The harmonic amplitude decreases sharply with the increase in the number of harmonics. The $2f$ signal has the highest amplitude among the even harmonic signals. The line shape is symmetrical with the absorption peak as the center.[19,21–23] The modulation depth is expressed as $m = \delta\nu/\Delta\nu$, where $\Delta\nu$ denotes the half-width at half maximum (HWHM) of the absorption spectrum line. Thus, the second harmonic component of the signal is often used for concentration inversion.

3. Experimental setup

The structure of the proposed simultaneous two-component gas detection RF-WM-OA-ICOS system is shown in Fig. 1. The system comprises an optical cavity composed of a self-designed stainless-steel cavity and two built-in spherical lenses with a reflectance of 99.999%, a diameter of 25.4 mm and a curvature radius of 1 m. The off-axis incident optical fiber frame, focusing lens, high-pass filter, and detector are integrated with a cage structure produced by Thorlabs. The laser sources include 1603 nm and 1653 nm distributed feedback (DFB) lasers, with the temperature and current controlled using Thorlabs TED200C & LDC202C and SRS Model LDC501 laser controllers, respectively. The two laser beams are coupled into one laser beam using a 2×1 fiber combiner and applied incident to the 26-cm optical cavity using a fiber collimator. The absorption lines corresponding to CH_4 and CO_2 are near 6046.96 cm^{-1} and 6243.91 cm^{-1}, respectively. The center temperature and current of the laser used for CO_2 measurement are 21.5 °C and 72 mA, respectively. The operating center temperature and current of the laser used for CH_4 measurement are 19.5 °C and 77 mA, respectively. The RF noise source coupled with the DFB lasers using a Bias-T

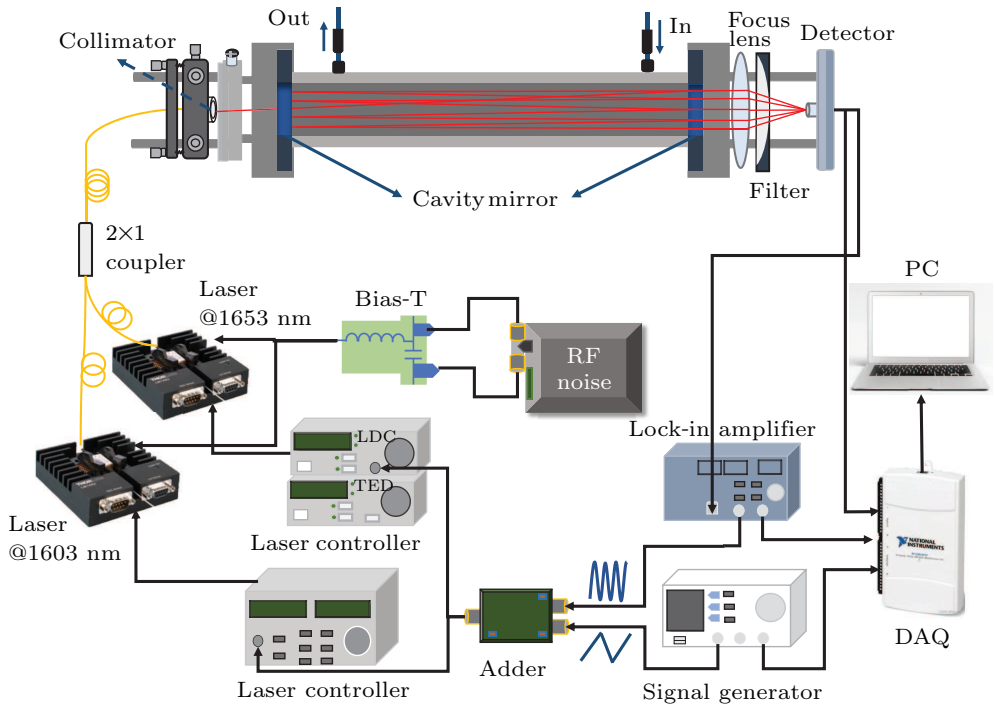


Fig. 1. Structure of the as-designed RF-WM-OA-ICOS simultaneous two-component gas detection system.

(Thorlabs, LM14S2-BT) to increase the linewidth of the output laser. A high-frequency sine wave generated by a phase-locked amplifier (SRS, SR830) and a low-frequency triangle wave generated by a signal generator (REGOL, DG1062) are superimposed using an adder and input to the laser controller for wavelength scanning. The output spectral signal is collected by a detector and transmitted to a lock-in amplifier for signal demodulation. The demodulated $2f$ signal is transmitted to the computer by using a DAQ (National Instruments, USB-6210) for gas concentration inversion. An experiment was performed using the proposed system with a sample gas mixture with gases of various concentrations prepared using a gas distribution system with a volume fraction of 2 ppm for CH_4 standard gas, 1020 ppm for CO_2 standard gas, and high-purity N_2 gas.

4. Experimental results and discussion

4.1. Experimental of two-channel signal coupling

First, the superimposed signal composed of two direct absorption signals from the cavity were analyzed based on the integrated cavity structure and optical path design. The direct absorption signals of CH_4 and CO_2 gases were measured by simultaneously injecting 1.0-ppm CH_4 and 510-ppm CO_2 gas into the cavity using the gas distribution system while maintaining the cavity pressure and temperature at 75 Torr (1 Torr = 1.33322×10^2 Pa) and 23 °C, respectively. The lasers were scanned using a triangular wave with a frequency of 50 Hz and an amplitude of 1.5 V; the results are shown in Fig. 2. The center currents of the two lasers were respectively varied upward (CO_2) and downward (CH_4) to measure the off-center wavelengths of the two gas-absorption signals and ensure that the two signals would not interfere with each other upon superposition (as shown in Figs. 2(b) and 2(c)). Then, the two laser signals were combined using the coupler and applied incident to the OA-ICOS cavity; the output signal is shown in Fig. 2(d). The two absorption peak positions in the output signal appeared in the first and second halves of the falling edge of the same triangular wave, indicating that the absorption signals of the two gases did not interfere with each other. With the modulation parameters used in the direct absorption signal experiment held constant, a sine wave signal with a frequency of 1.5 kHz was generated using a phase locked amplifier and superimposed on a low-frequency triangular wave signal (as shown in Fig. 2(e)) to conduct wavelength modulation experiments. The $2f$ signals of CH_4 and CO_2 after wavelength modulation were distributed at the left and right ends, as shown in Figs. 2(f) and 2(g), respectively. The $2f$ signals of the combined beam are shown in Fig. 2(h). Because the two lasers were modulated at the same modulation parameters, the output signal received by the detector was transmitted to the same lock-in amplifier for demodulation, and the harmonic signals of the two gases were obtained. The output signal was demodulated from the superposition of the two groups of absorption signals (as shown in Fig. 2(d)); thus, the two lasers were equivalent to each other's background signals. Therefore, the intensities of the obtained absorption spectra signal and the $2f$ signal were halved. However, this change in signal intensity did not affect the linear relationship between the intensity of the $2f$ signal and the concentrations of the two gases.

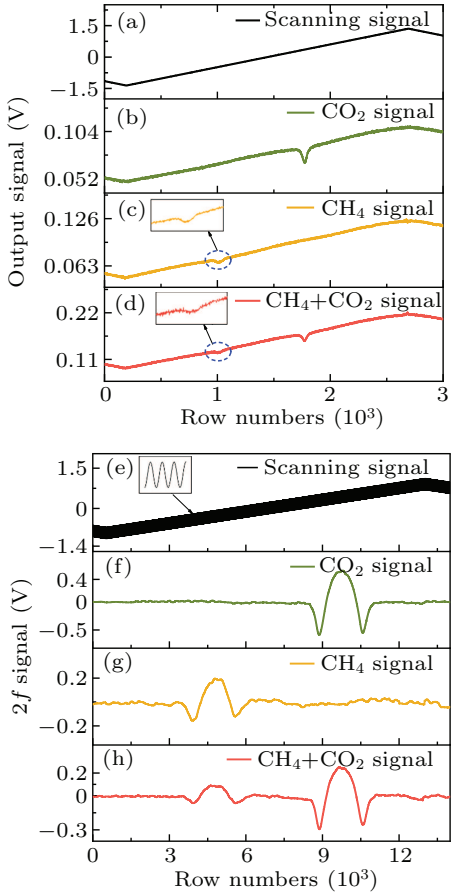


Fig. 2. (a) Direct absorption scanning signal, (b) CO_2 single direct absorption signal, (c) CH_4 single direct absorption signal, (d) CO_2 and CH_4 simultaneously absorb signals, (e) $2f$ scanning signal, (f) separately detected $2f$ signal of CO_2, (g) separately detected $2f$ signal of CH_4, (h) simultaneously detected $2f$ signals of CO_2 and CH_4.

4.2. Modulation signal parameters optimization

The spectral absorption signals of gases under the influence of different power RF noises were analyzed. Many experimental studies[24] have reported that the maximum second harmonic signal can be obtained when the modulation depth is 2.2. The HWHM of absorption spectrum signals was calculated in the present study, and the best modulation amplitude was 0.058212 cm^{-1}. Based on the relationship between the laser and the current, the optimal modulation current and the optimal modulation voltage were calculated as 6.0764 mA and 243.06 mV.

This study analyzed the $2f$ signals corresponding to the simultaneous absorption of CO_2 and CH_4 at 927 ppm and

4.55 ppm, respectively, under the influence of RF noise signals with different power values. The two laser controllers were modulated simultaneously using a triangular wave with a frequency of 1 Hz and amplitude of 2 V superimposed on a sine wave with a frequency of 1.8 kHz and an amplitude of 0.243 V; the RF noise was injected into the laser through the Bias-T. The RF noise source was variable from −10 dBm to −40 dBm, and the experimental design noise powers were −10 dBm, −15 dBm, −20 dBm, −25 dBm, −30 dBm, −35 dBm, and −40 dBm. The experimental results are shown in Fig. 3. During the measurements, the pressure and temperature in the cavity were 75 Torr and 23 °C, respectively.

As illustrated in Fig. 3(a), the original $2f$ signals contained a considerable amount of noise without RF noise perturbation, and regular noise distribution indicated that the noises originated from the cavity mode noise. This can be attributed to the minimal integrated cavity design. When RF noise was introduced, the cavity mode was notably suppressed. The same phenomenon occurred in the $2f$ spectra of both CH_4 and CO_2. With the increase in the noise power, all the cavity mode noises on the $2f$ spectra were notably suppressed, and the baseline was smooth. However, with the increase in noise power, the $2f$ peaks exhibited severe distortion, the spectral peak value decreased gradually, and the spectral line widened gradually. The deformation of the $2f$ peaks was not prominent when the RF power was lower than −20 dBm. When the noise power was higher than −20 dBm, the peak value decreased, and the trough value gradually increased and shifted away from the peak center.

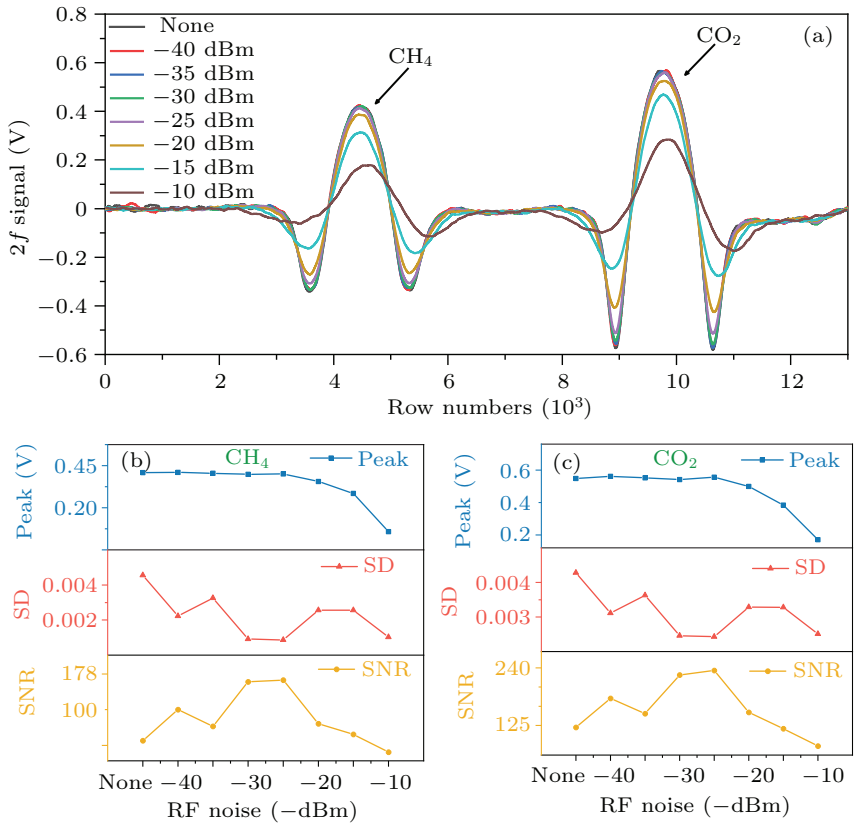


Fig. 3. (a) Simultaneous detection of $2f$ signals of CH_4 and CO_2 with different noise power disturbances, (b) parameters of the CH_4 $2f$ signal, (c) parameters of the CO_2 $2f$ signal.

The peak amplitude, SNR, and SD corresponding to CH_4 and CO_2 signals under the influence of different noise power were calculated according to $2f$ signals, as shown in Figs. 3(b) and 3(c). The peak amplitude decreased gradually with the increase in noise power. However, the SNR first increased and then decreased with noise power. When the noise power was −25 dBm, the SNR and SD reached the maximum and minimum values, respectively. The SNRs of the two groups of gas signals were approximately 174 and 231, respectively, which were 1.8 times the values obtained when noise disturbance was absent, and the corresponding SD values were small. Therefore, −25 dBm was determined as the optimal RF level for enhancing the system in the following experiment.

4.3. System concentration calibration experiment

The response relationship and measurement accuracy of the RF-WM-OA-ICOS system to the concentrations of two gases were evaluated through a series of measurements of mixed gases of different concentrations. The gases included 2.0 ppm of CH_4 standard gas, 1020 ppm of CO_2 standard gas, and high-purity nitrogen gas. The $2f$ signals of the two gases were evaluated simultaneously through continuous in-

let and dynamic measurements. Data of the original signals were recorded every 20 times on average. The relationship between the concentrations of CH_4 and CO_2 and the $2f$ signal amplitude was investigated, and the results are shown in Fig. 4(a). The left absorption spectrum peak corresponded to CH_4, and the right spectrum peak corresponded to CO_2. The peaks of the collected CH_4 and CO_2 $2f$ signals indicated a strong linear correlation of CH_4 within a concentration of approximately 2.0 ppm. The square of the correlation coefficient is 0.99979. The CH_4 concentration (C_{CH4}) and the peak amplitude of the $2f$ signal (A_{2f1}) exhibit a linear relationship as follows:

$$C_{CH_4} = -0.01789 + 0.101013 \cdot A_{2f1}. \tag{7}$$

The square of the polynomial correlation coefficient corresponding to a CO_2 concentration of approximately 1020 ppm is 0.99984, and CO_2 concentration (C_{CO2}) and the peak amplitude of the $2f$ signal (A_{2f2}) exhibit a nonlinear relationship as follows:

$$C_{CO_2} = 0.02706 + 7.126 \times 10^{-4} \cdot A_{2f2} - 1.77 \times 10^{-7} \cdot A_{2f2}^2. \tag{8}$$

The relationship between C_{CO2} and A_{2f2} is nonlinear because the relationship between the absorption coefficient of the gas and the single-pass absorption loss did not satisfy the weak absorption conditions of the off-axis integration cavity. In the measurement environment with a pressure and temperature of 75 Torr and 23 °C, respectively, the HITRAN database was used to simulate the absorption coefficient of CO_2 at 6043.91 cm^{-1}. The absorption coefficient for CO_2 with a volume fraction of 1020 ppm was 3.6×10^{-5} cm^{-1}. The reflectivity of the lens used was approximately 99.999%, and the cavity mirror spacing (d) is approximately 26 cm. Therefore, the one-way absorption loss is $\alpha_{CO_2} \times 26 = 9.36 \times 10^{-4}$, while the single reflection loss of the mirrors is $1 - R = 10^{-5}$, which is not satisfied when $\alpha_{CO_2} L_c \ll 1 - R$. Thus, a curved relationship was observed within the concentration range.

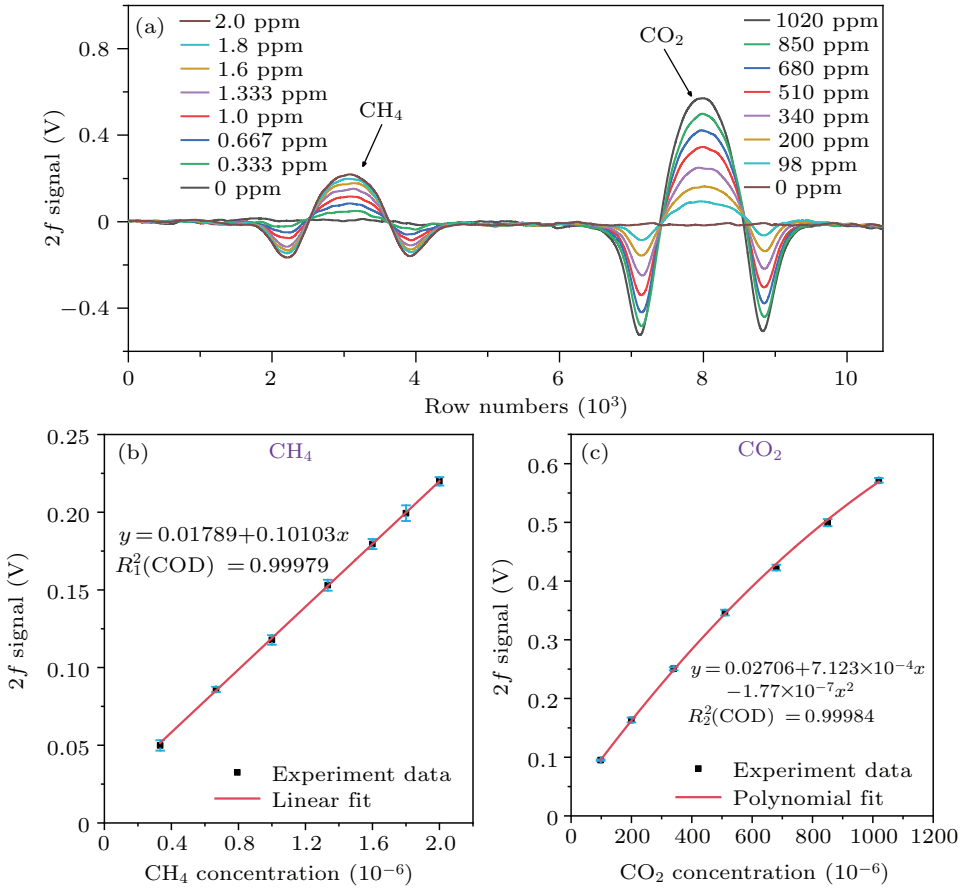


Fig. 4. (a) Simultaneous detection of $2f$ signals for multiple groups of CH_4 and CO_2, (b) $2f$ signal for 0–2.0 ppm of CH_4, (c) $2f$ signal for 0–1020 ppm of CO_2.

4.4. System performance analysis

Through the gas distribution system, 2.0-ppm CH_4 and 340-ppm CO_2 were injected into the cavity through the gas distribution system to analyze the stability and measurement accuracy of the system; continuous measurements were recorded for approximately 40 min. The RF-WM-OA-ICOS method with a noise disturbance of −25 dBm was adopted for data acquisition. The amplitude value was substituted into

the above fitting formula for concentration inversion. The signals for single data recording were acquired with an integration time of 1 s. The results for CH_4 and CO_2 are shown in Figs. 5(a) and 5(c), respectively. Data analysis and Allan variance analysis[25] were performed using the results. The average measured concentrations of CH_4 and CO_2 were 1.97 ppm and 340.58 ppm, respectively, indicating accuracies of 1.5% and 0.17%, respectively, with standard deviations of 0.1424 ppm and 27.733 ppm, indicating that the differences were within acceptable error limits.

As illustrated in Figs. 5(c) and 5(d), the minimum detectable concentrations of CH_4 and CO_2 were 0.14 ppm and 27.2 ppm within an integration time of 1 s. When the systematic integration time was 1 min, the minimum detectable concentrations decreased to 19 ppb and 3.7 ppm, respectively. The optimal integral times of the system for CH_4 and CO_2 detection are 220 s and 458 s, respectively, with corresponding minimum detectable concentration limits of 10 ppb and 1.345 ppm, respectively. For the entire system, 220 s can be regarded as the optimal integration time. Within this integration time, the minimum detectable concentration limits of CH_4 and CO_2 are 10 ppb and 1.50 ppm. Using the method proposed by Moyer *et al.*[26] based on the sampling integration time and the corresponding minimum detectable absorption factor, the corresponding noise equivalent absorption sensitivity (NEAS) was calculated as 2.67×10^{-13} $cm^{-1}\cdot Hz^{-1/2}$ and 5.18×10^{-11} $cm^{-1}\cdot Hz^{-1/2}$.

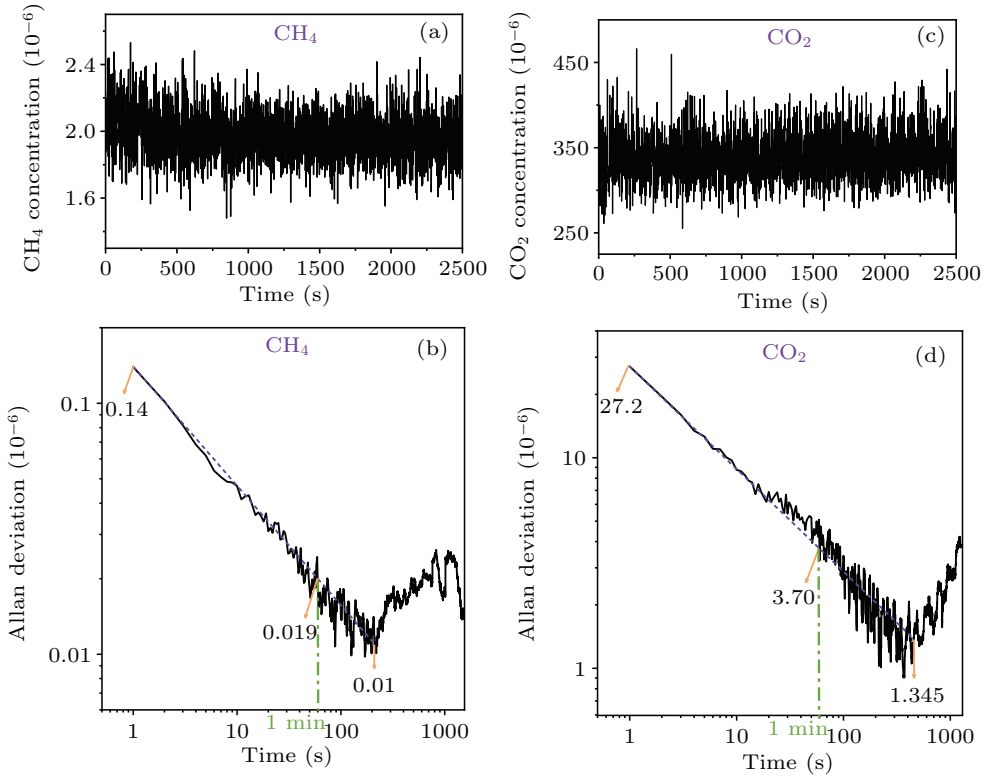


Fig. 5. (a) Time-series measurements for CH_4 at a constant concentration of 2 ppm over approximately 40 min, (b) Allan variance of CH_4, (c) time-series measurements for CO_2 at a constant concentration of 340 ppm over approximately 40 min, (d) Allan variance of CO_2.

5. Conclusions

This study designed a novel high-precision system for the simultaneous detection of CH_4 and CO_2 through RF-WM-OA-ICOS with a beam combiner. The stability of the system was investigated after the optimization of the modulation parameters of the system and the calibration of the relationship between the $2f$ signals and concentration. The results indicated that the system has high stability and can be used to accurately and simultaneously measure the concentrations of CH_4 and CO_2. The optimal integration time of the system is 220 s. The minimum detection limit of CH_4 is 10 ppb, and that of CO_2 is 1.5 ppm. The corresponding NEAS values were calculated as 2.67×10^{-13} $cm^{-1}\cdot Hz^{-1/2}$ and 5.18×10^{-11} $cm^{-1}\cdot Hz^{-1/2}$, respectively. Therefore, the proposed dual-component gas simultaneous detection method can achieve high measurement accuracy, has a simple structure, and is easy to implement. It can be used for high-precision simultaneous detection of other gases and can serve as a basis for the development of portable multicomponent gas analyzers.

Acknowledgements

Project supported by the National Natural Science Foundation of China (Grant Nos. 62005108 and 62205134), the National Key Research and Development Program of China (Grant No. 2022YFC2807701), and the Natural Science Foundation of the Higher Education Institutions of

Jiangsu Province, China (Grant Nos. 20KJB140009 and 21KJB140008).

References

[1] Pan B H 2022 *Ecological Economy* **38** 1
[2] Qu J S, Chen W, Zeng J J, Sun Y L, Liao Q, Guo K M, Qin A N, Pei H J, Teng F, Liu Y F, Yue F, Liu L N, Tang Y and Li L C 2022 *Bull. Chin. Acad. Sci.* **37** 444
[3] Nadeem F, Mandon J, Cristescu S M and Harren F J M 2018 *Appl. Opt.* **57** 29
[4] Stewart G 2021 *Laser and Fiber Optic Gas Absorption Spectroscopy* (Cambridge: Cambridge University Press) p. 125
[5] Ciaffoni L, Couper J, Hancock G, Peverall R, Robbins P A and Ritchie G A D 2014 *Opt. Express* **22** 17030
[6] Manfred K M, Kirkbride J M R, Ciaffoni L, Peverall R and Ritchie G A D 2014 *Opt. Lett.* **39** 6811
[7] Shao L, Chen J, Wang K, Mei J, Tan T, Wang G, Liu K and Gao X 2022 *Sensor. Actuat. B-Chem.* **352** 130995
[8] Kasyutich V L, Canosa-Mas C E, Pfrang C, Vaughan S and Wayne R P 2002 *Appl. Phys. B* **75** 755
[9] Zhao W, Gao X, Chen W, Zhang W, Huang T, Wu T and Cha H 2007 *Appl. Phys. B* **86** 353
[10] Wang J, Tian X, Dong Y, Chen J and Gao X 2019 *Opt. Lett.* **44** 3298
[11] Dong Y, Wang J J, Zhou X Y, Zhu G D, Qu K, Wu X E, Lv W J, Wen M M, Tan T and Liu K 2020 *Chin. J. Lasers* **47** 0811003
[12] Wang K, Shao L, Chen J, Wang G, Liu K, Tan T, Mei J, Chen W and Gao X 2020 *Sensors* **20** 21
[13] Gagliardi G and Loock H P 2014 *Cavity-enhanced spectroscopy and sensing* (Heidelberg: Springer) p. 16
[14] Chao X, Shen G, Sun K, Wang Z, Meng Q, Wang S and Hanson R K 2019 *P. Combust. Inst.* **37** 1345
[15] Engel G S, Moyer E J, Keutsch F N and Anderson J G 2001 *Proceedings of the NASA Earth Science Technology Conference (ESTC)*, College Park, MD, USA, p. 28
[16] Pinto T H P, Kirkbride J M R and Ritchie G A D 2018 *Opt. Lett.* **43** 1931
[17] Stéphan G M, Tam T T, Blin S, Besnard P and Têtu M 2005 *Phys. Rev. A* **71** 043809
[18] Wang J J, Dong Y, Tian X, Chen J J, Tan T, Zhu G D, Mei J X and Gao X M 2020 *Spectrosc. Spect. Anal.* **40** 2657
[19] Wang G, Mei J, Tian X, Liu K, Tan T, Chen W and Gao X 2019 *Opt. Express* **27** 4878
[20] Philippe L C and Hanson R K 1993 *Appl. Opt.* **32** 6090
[21] Kluczynski P, Gustafsson J, Lindberg S M and Axner O 2001 *Spectrochim. Acta B* **56** 1277
[22] Reid J and Labrie D 1981 *Appl. Phys. B* **26** 203
[23] Schilt S, Thévenaz L and Robert P 2003 *Appl. Opt.* **42** 6728
[24] Chakraborty A L, Ruxton K and Johnstone W 2010 *Opt. Lett.* **35** 2400
[25] Liu J T C, Jeffries J B and Hanson R K 2004 *Appl. Phys. B* **78** 503
[26] Moyer E J, Sayres D S, Engel G S, Clair J M St, Keutsch F N, Allen N T, Kroll J H and Anderson J G 2008 *Appl. Phys.* **92** 467